Effect of Intramolecular Cycles on the Polycyclotrimerization of Aromatic Dicyanates

RONG-HSIEN LIN,[1] AN-CHUNG SU,[2] JIN-LONG HONG[2]

[1] Department of Chemical Engineering, National Kaohsiung Institute of Technology, Kaohsiung 80782, Taiwan

[2] Institute of Material Science and Engineering, National Sun Yat-Sen University, Kaohsiung 80424, Taiwan

Received 21 October 1998; accepted 13 January 1999

ABSTRACT: The gel conversions (α_{gel}) for the polycyclotrimerization of aromatic dicyanates are significantly higher than the classical mean-field value of 0.5. The reasons for the higher gel conversion, which is consistent with all experimental results of different structures of monomers, were inductively attributed to the accessibility effect of the functional group and the substitution effect, as well as the effect of the intramolecular cyclization. Nevertheless, the former two effects on the gel conversion can be quantitatively represented in terms of the extent of the intramolecular cyclization. Some theoretical expressions (including gel conversion and crosslink density with respect to the conversion) were derived by use of the recursive method with due consideration of the intramolecular cyclization. These expressions (with only one experimental parameter, α_{gel}) were found to be effective in describing gel fraction–conversion data for various polycyanurates. A dramatic change in the product value of $\Delta C_p \cdot T_g$ was also found in the vicinity of the gel point for all different structures of aromatic dicyanate systems. The dramatic change in $\Delta C_p \cdot T_g$ occurs at the gel point rather than the expected mean-field gel conversion of 0.5, presumably due to the intramolecular cyclization. © 1999 John Wiley & Sons, Inc. J Appl Polym Sci 73: 1927–1938, 1999

Key words: aromatic dicyanate; gel conversion; intramolecular cyclization

INTRODUCTION

Polycyclotrimerization of aromatic dicyanates proceeds via a combination of three functional groups to form a triazine ring as a junction point, as illustrated in Scheme 1. Only one type of linkage (triazine ring) is formed during the full course of the polycyclotrimerization. Gelation in the polycyclotrimerization of aromatic dicyanates have been of great interest due to practical as well as theoretical interests. The mean-field prediction of gel conversion for these systems is 0.5.[1] This was shown using either the recursive method[1,2] or the expression derived by Fukui and Yamabe.[3] The mean-field theory, however, does not accurately predict the gel conversion of tightly branched, rigid polycyanurates. The reports of the gel conversion for several different aromatic dicyanates in the literature[1,4–14] were found to be between 0.58 and 0.65, except the result of 0.52–0.54 in the flexible long chain system,[15] exhibiting significant higher values than the predicted gel conversion. These delayed gel conversions were inductively attributed to the absorbed water,[4] the effect of global diffusion,[1,16] the accessibility of the functional group,[1,17,18] and the substitution

Correspondence to: R.-H. Lin.

Contract grant sponsor: National Science Council; contract grant number: NSC-87-2216-E-151-002.

Journal of Applied Polymer Science, Vol. 73, 1927–1938 (1999)

 CCC 0021-8995/99/101927-12

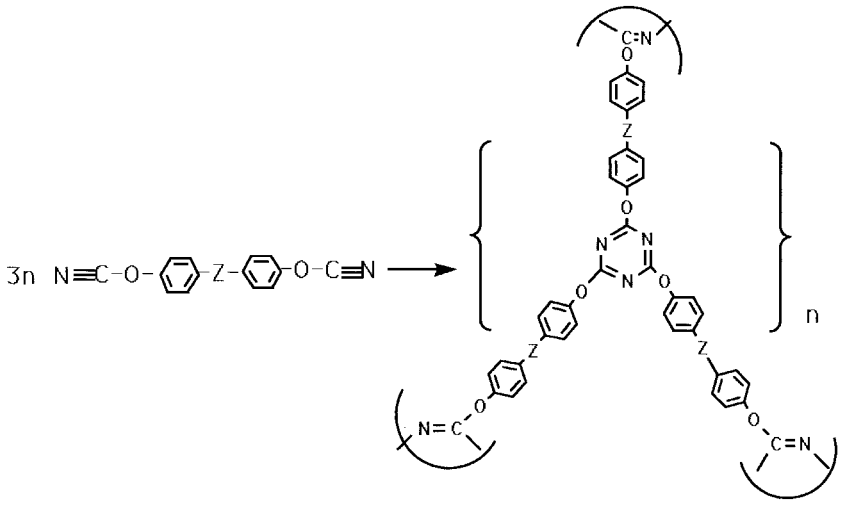

Scheme 1 Polycyclotrimerization of aromatic dicyanate to form a *sym*-triazine structure.

effect,[1,19] as well as the effect of the intramolecular cyclization.[1,17,18,20,21]

Georjon et al.[4] suggested that the delayed gel conversion occurs due to the formation of the linear structure during the polycyclotrimerization in the presence of moisture. The functional groups are thus wasted due to no branching point (*sym*-triazine ring) forming, thereby delaying the gel conversion. Experimentally, no significant linear structure was found during the polycyclotrimerization via ^{1}H nuclear magnetic resonance (NMR) and infrared (IR) observations.[1,22,23] On the other hand, the recursive method[2] indicated that there must be at least one mole H_2O required to react with two moles dicyanates to delay the gel conversion to 0.64. It seems impossible to absorb so much of water in this system (actually, all experimental specimens were sealed in hermetic pans). Therefore, the effect of the absorbed water should be excluded.

Gupta and Macosko[1] suggested that the substitution effect of aromatic dicyanate does not apparently affect the gel conversion because the two cyanate functional groups on various aromatic dicyanate systems studied in the literature are sufficiently separated on the corresponding monomer. However, if an electron-withdrawing group on the backbone of aromatic dicyanate monomer exists, the substitution effect arises when one of the two cyanate functional groups on aromatic dicyanate has been reacted.

In our opinion, accessibility of the functional group, the substitution effect, and the effect of the intramolecular cyclization are not independent events. The former two effects more or less influence the extent of intramolecular cyclization. Accordingly, the former two effects on the gel conversion may be profoundly associated with the extent of the intramolecular cyclization. Intramolecular cyclization, therefore, may play a dominant role in the dramatic change in physical properties (gel conversion, elastically effective crosslink density, or the product value of $\Delta C_p \cdot T_g$).

Simha and Boyer[24,25] derived a relationship from the free volume theory as follows:

$$(\alpha_R - \alpha_G)T_g = \Delta\alpha \cdot T_g = \mathrm{V_{f,g}} = \mathrm{K_1} \qquad (1)$$

where α_R and α_G represent the volume expansion coefficients in the rubbery and glassy states, respectively. $\mathrm{V_{f,g}}$ is the free volume at the glass transition temperature. They also made a conclusion that free volume at the glass transition temperature ($\mathrm{V_{f,g}}$) is indeed a constant, 11.3%.

Using the hole theory from kinetic aspect, Nose[26,27] examined the change in heat capacity, ΔC_p, and derived the general relationship at the glass transition temperature, as follows:

$$\frac{T_g V(\Delta\alpha)^2}{\Delta C_p \cdot \Delta\beta} = 1 \qquad (2)$$

where $\Delta\alpha$ and $\Delta\beta$ refer to the differences in the thermal expansion coefficient and compressibility between the liquid (rubbery) and glassy state, respectively. V is the volume of material. Substituting eq. (1) into eq. (2), we obtain

$$\Delta C_p \cdot T_g = K_1^2 V/\Delta\beta \quad (3)$$

The left-hand side would be constant if $(V/\Delta\beta)$ were a constant for all polymers. Using the tabulation of Wunderlich,[28] this product $(\Delta C_p \cdot T_g)$ ranges in values from 80 to 140 J/g, with 7 of the 12 values in the range of 105 ± 13 J/g. Richardson and Savill[29] examined an anionic polystyrene sample and found that $\Delta C_p \cdot T_g$ is approximately equal to 109 ± 5 J/g.

It is instructive to check whether $\Delta C_p \cdot T_g$ remains unaltered during the whole course of polycyclotrimerization of aromatic dicyanate. If discontinuity arises in between the whole conversion range from $\alpha = 0$ to $\alpha = 1$, then where is the most likely to happen, and what are the probable reasons? It is of some interest to know whether intramolecular cyclization plays a significant role in the property of $\Delta C_p \cdot T_g$.

Some aromatic dicyanates with special structure are deliberately designed and synthesized for the further study in the remaining unclear subjects.

EXPERIMENTAL

Material

Bisphenol-A dicyanate (BADC), 4,4′-thiodiphenylcyanate (TDPC), tetramethylbisphenol-A dicyanate (TMBADC), 2,2-bis(4′-cyanatophenyl)hexafluoropropane (HFBADC), and cyanated phenylene sebacate (CPS) were synthesized from the corresponding diol compounds according to the cyanogen method.[22,30] The crude product was further purified via consecutive recrystallization with hot carbon tetrachloride or chloroform before characterization by means of ^{1}H-NMR, Fourier transform infrared (FTIR), and elemental analysis (EA). Precursor material, hydroxyl-terminated phenylene sebacate, for CPS was usually found as an oligomer after being synthesized from the hydroquinone and sebacoyl chloride; hence, CPS was also an oligomer (with $n = 1.2$ in the following indicated structure).

BADC: 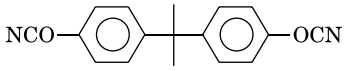

TDPC: 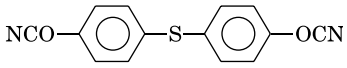

TMBADC: 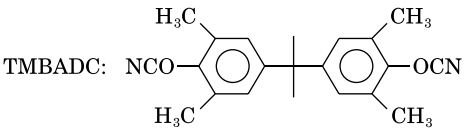

HFBADC: 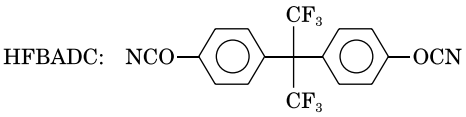

CPS: 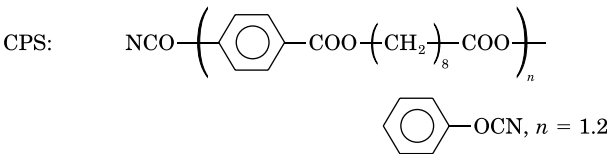

Methods

Isothermal Cure

Two TDPC samples (one approximately 7 mg; the other one, approximately 30 mg) sealed in hermetic pans were simultaneously put into the DSC cell every time and cured isothermally at different temperatures (150, 160, and 180°C) for various periods of time to the desired extent of reaction, then immediately quenched with liquid nitrogen to room temperature. The smaller sample was subsequently rescanned at a heating rate of 20°C/min to measure the residual heat ΔH_{res} and, hence, the extent of reaction (α). The larger sample was dissolved in CH_2Cl_2 and shaken for 6 days before determination of gel fraction via gravimetry.

Dynamic Cure

Two samples (one approximately 7 mg; the other one approximately 10–15 mg) for various specimens sealed in hermetic pans were simultaneously put into the DSC cell every time and cured at a heating rate of 20°C/min to the desired temperature (and, hence, the desired extent of reaction), then immediately quenched with liquid nitrogen. Determinations of ΔH_{res} and the gel fraction were similar to their counterparts in the isothermal case, except that the TMBADC sample was dissolved in THF instead of in CH_2Cl_2.

Determination of T_g and ΔC_p

Samples approximately 5–7 mg in weight were sealed in hermetic pans and cured in a differential scanning calorimetry (DSC) cell at a heating rate of 20°C/min to the desired temperature (and, hence, the desired extent of reaction, $\alpha < 0.6$), then immediately quenched with liquid nitrogen,

and, finally, subsequently heated at a rate of 20°C/min to measure T_g and ΔH_{res}. For the high conversion samples ($\alpha \geq 0.6$), air cooling instead of liquid nitrogen quenching was adopted; and before DSC scanning to measure T_g and ΔH_{res}, additional long-term (more than 15 days) physical aging procedure at room temperature was taken to make the T_g apparent to be observed. The corresponding jump in heat capacity across T_g was taken as ΔC_p.

Two-point calibration (In/Zn for the high-temperature runs and In/EA for the low-temperature) of DSC was regularly performed. A stream of high-purity nitrogen at a flow rate of 20 mL/min was used to purge the DSC cell. Conversion (α) was calculated by $\alpha = 1 - \Delta H_{res}/\Delta H_{tot}$, where ΔH_{tot} is the total evolved energy when the sample was heated to complete cure from monomer. T_g was taken as the temperature at the midpoint of the transition region. The gravimetric procedure in gel fraction determination was proceeded by filtrating the dissolved solution by means of glass-fiber filter paper (0.6-μm pore size) and subsequently drying the filtrated sample to constant weight. A blank experiment was performed for correction of residual sample weight when the solvent was being dried from the filter paper.

THEORY

For the sake of clarity, brief derivations for properties under the classical mean-field assumption are given before the development of corresponding expressions in the presence of intramolecular cycles. This serves to provide direct comparisons of fitting data between the classical and the present approaches.

Expressions under Mean-Field Assumption

According to the recursive method of Macosko and Miller,[2,31] the gel fraction (ϕ_{gel}) and crosslink density (X) at a certain conversion level α in the post-gel regime may be derived as follows. As illustrated in Scheme 2(a), the probability of finding a finite chain when looking outwards from a cyanate group C, $P(F_{out})$, is related to that when looking inwards, $P(F_{in})$, by the following relationship:

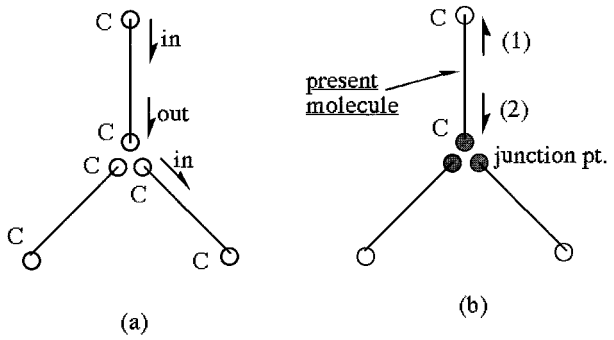

Scheme 2 Schematic representation of the reacting status of monomer segments.

$$P(F_{out}) = P(F_{out}|C \text{ reacted}) \cdot P(C \text{ reacted}) + P(F_{out}|C \text{ unreacted}) \cdot P(C \text{ unreacted}) = [P(F_{in})]^2 \cdot \alpha + 1(1 - \alpha) \quad (4)$$

Since $P(F_{out}) = P(F_{in})$, we obtain

$$P(F_{out}) = (1 - \alpha)/\alpha \quad (5)$$

If the crosslink density X_{SG} is defined as "the fraction of the junction points whose three arms are part of the infinite gel network" (definition of Simon and Gillham[32]), as illustrated in Scheme 2(b), one may write

$$X_{SG} = (1 - P(F_{out})) \xrightarrow{\text{path(1)}} \{(1 - P(F_{out}))^2 \alpha\} \xrightarrow{\text{path(2)}} \frac{C_o/3}{C_o}$$

$$= \alpha(1 - P(F_{out}))^3/3$$

$$= (\tfrac{1}{3})\alpha(2 - 1/\alpha)^3 \quad (6)$$

If X is defined as "the fraction of segments that are crosslinked," the definition of the so-called original DiBenedetto equation[33] and HMB equation,[34] we have

$$X = \alpha(1 - P(F_{out}))^3 = \alpha(2 - 1/\alpha)^3 \quad (7)$$

On the other hand, we have the sol fraction ϕ_{sol} as

$$\phi_{sol} = [P(F_{out})]^2$$

and, hence, the gel fraction beyond the gel point is expressed as

$$\phi_{gel} = 1 - [P(F_{out})]^2 = 1 - [(1 - \alpha)/\alpha]^2 \quad (8)$$

The gel point, which corresponds to the threshold conversion that $\phi_{gel} \to 0$ and $X \to 0$, is therefore located at $\alpha_{gel} = 0.5$ from eqs. (7) and (8), and we have $X = 0$ and $\phi_{gel} = 0$ when $\alpha \leq \alpha_{gel}$.

Expressions Considering the Effect of Intramolecular Loops

Using the recursive approach, we[35] had strictly derived expressions in detail considering the effect of intramolecular cycles in the polycyclotrimerization of dicyanate systems. The gel fraction ϕ_{gel} had been expressed as

$$\phi_{gel} = 1 - (1 - 2f\alpha + f^2\alpha)^2(f^2\alpha)^{-2} \qquad (\alpha > \alpha_{gel}) \quad (9)$$

where f is the probability that an incoming cyanate group is from a different cluster (i.e., without forming intramolecular loop). We suggested that f should generally increase with conversion in the post-gel regime due to combined (and, yet, opposite) effects from intramolecular cyclization and loop-interlocking and is expressed as follows:

$$f(\alpha) = 1 - [1 - (2\alpha_{gel})^{-1}][(1 - \alpha)/(1 - \alpha_{gel})]^m \qquad (\alpha > \alpha_{gel}) \quad (10)$$

where m is an adjustable parameter.

Equations (9) and (10) and the equation derived therefrom for crosslink density are actually not practical and too complicated. Therefore, we attempt to derive simpler expressions from another approach. Extent of the intramolecular cycles in the post-gel regime may be regarded presumably as constant due to the fact that the effect of loop-interlocking on the gel fraction is not significantly observed in that regime. Based on this assumption, the expressions may be derived as the following. Although intramolecular cycles are infinitely recursive, they are still considered as finite chains, as illustrated in Scheme 3 (each junction is a sym-triazine ring). We introduced a parameter b ($b \geq 1$) to modify the probability of finite chain. Therefore, we have

$$\phi_{gel} = 1 - [b \cdot P(F_{out})]^2 = 1 - [b \cdot (1 - \alpha)/\alpha]^2 \quad (11)$$

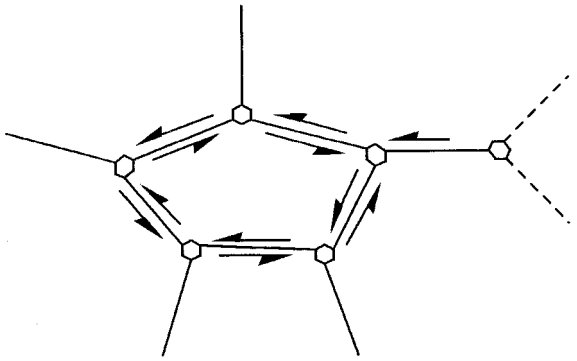

Scheme 3 Schematic illustration of the intramolecular loop. It is infinitely recursive but is still considered as a finite chain. Each junction is a *sym*-triazine ring.

The boundary condition that $\phi_{gel} = 0$ as $\alpha = \alpha_{gel}$ leads to $b(\alpha = \alpha_{gel}) = \alpha_{gel}/(1 - \alpha_{gel})$; that is, the extent of intramolecular cyclization $g = [(b - 1)/b]/2 = 1 - \frac{1}{2}\alpha_{gel}$ is presumably unaltered beyond the gel point. The divisor is 2 because the loop was counted twice from the opposite direction. Another boundary condition that $\phi_{gel}(\alpha = 1) = 1$ is automatically satisfied. Equation (11) therefore becomes eq. (12), containing only one parameter (α_{gel}), which can be experimentally determined.

$$\phi_{gel} = 1 - [\alpha_{gel}/(1 - \alpha_{gel})]^2 \cdot [(1 - \alpha)/\alpha]^2 \qquad (\alpha > \alpha_{gel}) \quad (12)$$

With the same approach, the elastically effective crosslink density (X') was obtained by introducing a parameter b into eq. (7) due to the fact that crosslinked junction points within the intramolecular cycles are not elastically effective. Therefore, we have

$$X' = \alpha[1 - b \cdot P(F_{out})]^3. \quad (13)$$

The boundary condition that $X' = 0$ as $\alpha = \alpha_{gel}$ leads to $b(\alpha = \alpha_{gel}) = \alpha_{gel}/(1 - \alpha_{gel})$, which is the same value as above-determined due to the same physical meaning. Another boundary condition that $X'(\alpha = 1) = 1$ is again automatically satisfied. The corresponding expression for the elastically effective crosslink density is therefore

$$X' = \alpha\left(1 - \frac{\alpha_{gel}}{1 - \alpha_{gel}} \cdot \frac{1 - \alpha}{\alpha}\right)^3 = \alpha\left(\frac{1 - \alpha_{gel}/\alpha}{1 - \alpha_{gel}}\right)^3 \qquad (\alpha > \alpha_{gel}) \quad (14)$$

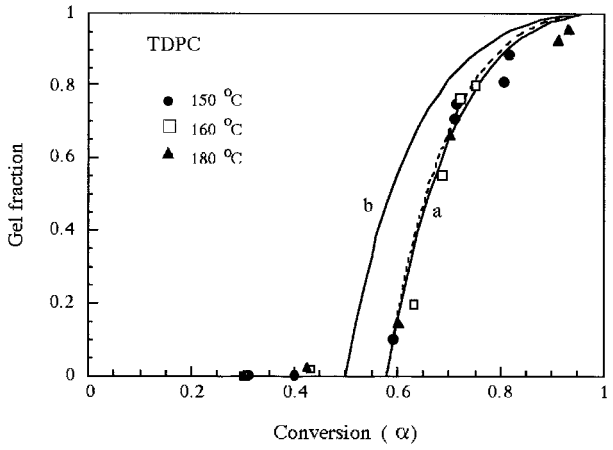

Figure 1 Comparisons between the calculated gel fraction curves and the experimental TDPC counterparts (symbols). The solid line (b) follows eq. (8); the solid line a represents eq. (12) with $\alpha_{gel} = 0.58$ and a dash line by using eqs. (9) and (10) and $m = 0.5$.

We have $X' = 0$ when $\alpha \leq \alpha_{gel}$.

The mean-field crosslink density (X) and the elastically effective crosslink density (X') had been applied to examine the influence on T_g-conversion dependence.[22] This subject is not discussed in this work.

RESULTS AND ANALYSIS

TDPC System and Effect of Global Diffusion

Reaction temperature can apparently influence the mobility of molecular mass center (global diffusion). The higher reaction temperature is employed, the higher global diffusion, and vice versa. To distinguish the effect of chain-end diffusion, we chose a shorter segment specimen, such as TDPC, to study the effect of global diffusion on the gel conversion (α_{gel}) at the various temperatures. Given in Figure 1 are ϕ_{gel}–α data gathered from all the isothermal cure data (150, 160, and 180°C). Within experimental uncertainties, a one-to-one ϕ_{gel}–α relationship was observed, irrespective to the cure temperature. It implies that the global diffusion is not a factor to change the gel conversion. Extrapolation of data indicated that the gel point is located at a conversion level of 0.58 ± 0.01. Figure 1 also shows the comparisons between the calculated gel fraction curves and the experimental counterparts (symbols). The solid line (b) follows eq. (8), which is under the mean-field assumption, illustrating a significant deviation from the experimental data. However, the solid line (a) [using eq. (12) with $\alpha_{gel} = 0.58$] and dash line [using eq. (9) and (10) and $m = 0.5$] exhibit the fact that there is no apparent discrepancy between these two equations and that both equations were in good agreement with data. Accordingly, eq. (12) will be thereafter utilized to predict the gel fraction. More importantly, it implies that the formation of intramolecular loops make no contribution to the gelation.

Dynamic cure data also gave $\alpha_{gel} = 0.58$ (not shown for brevity), matching the conclusion that the global diffusion is not a factor to change the gel conversion. Therefore, to save the experimental time, we adopted the dynamic cure method to determine the gel fraction (ϕ_{gel}) for the other specimens.

Effects of Accessibility, Substitution, and Intramolecular Cyclization in the Other Specimens

As compared with BADC, a specimen with less accessibility, such as TMBADC, a specimen that has higher accessibility, such as CPS, and a positive substitution effect specimen, such as HFBADC, were selected to make comparison of gel conversion (α_{gel}). The gel conversions for these dicyanate systems were determined by extrapolating the experimental data of the gel fraction to $\alpha_{gel} = 0$ and are summarized in Table I. Given in Figures 2–5 are the plots of gel fraction (ϕ_{gel}) versus conversion in the post-gel regime of polycyclotrimer-

Table I Summary of Gel Conversions (α_{gel}) in Different Cure Methods for Various Structures of Aromatic Dicyanates

α_{gel}	TDPC	HFBADC	TMBADC	BADC	CPS
Dynamic cured	0.58	0.55	0.62	0.60	0.52
Isothermal cured 150°C	0.58	—	—	—	—
Isothermal cured 160°C	0.58	—	—	—	—
Isothermal cured 180°C	0.58	—	—	—	—

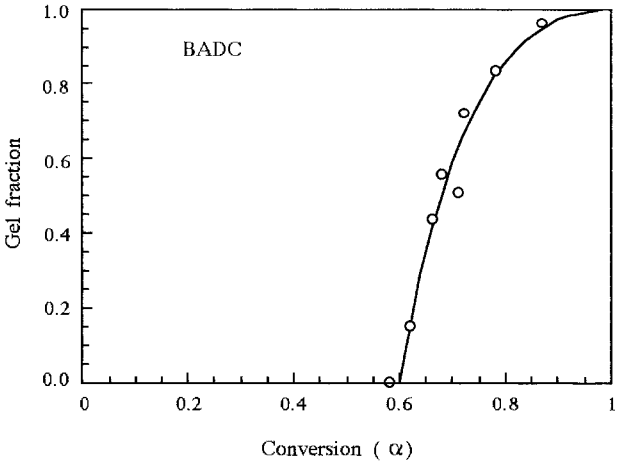

Figure 2 Comparisons between the calculated gel fraction curve and the experimental BADC counterparts (symbols). The solid line is the calculated gel fraction curve by means of eq. (12) and $\alpha_{gel} = 0.60$.

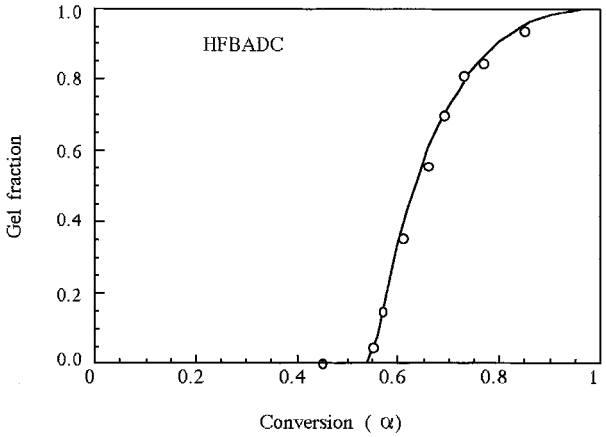

Figure 4 Comparisons between the calculated gel fraction curve and the experimental HFBADC counterparts (symbols). The solid line is the calculated gel fraction curve by means of eq. (12) and $\alpha_{gel} = 0.55$.

ization of BADC, TMBADC, HFBADC, and CPS, respectively. The solid lines are the calculated gel fraction curve by means of eq. (12) and the corresponding α_{gel}, exhibiting a good fit to the experimental counterparts (symbols).

Relationship of ΔC_p versus T_g

Generally, the product of $\Delta C_p \cdot T_g$ from the experimental observation is approximately constant for most of thermoplastic polymer,[28,29] irrespective of the molecular weight. But interestingly, $\Delta C_p \cdot T_g$ is not constant for whole range of conversion in the aromatic dicyanate system. Shown in Figures 6–9 are the plots of ΔC_p versus T_g for TDPC, BADC, TMBADC, and HFBADC, respectively. Within experimental uncertainties (indicated by error bar), there exists a dramatic discontinuity in the vicinity of gel conversion, indicating that the previously mentioned factor (formation of intramolecular loops) for the delayed gel conversion also have a significant effect on the change in the product value of $\Delta C_p \cdot T_g$. The solid line in the pre-gel regime was presented by one value of $\Delta C_p \cdot T_g$, whereas it is represented by another value of $\Delta C_p \cdot T_g$ in the post-gel regime. All of these values for various systems are summarized in Table II. Larger deviations were

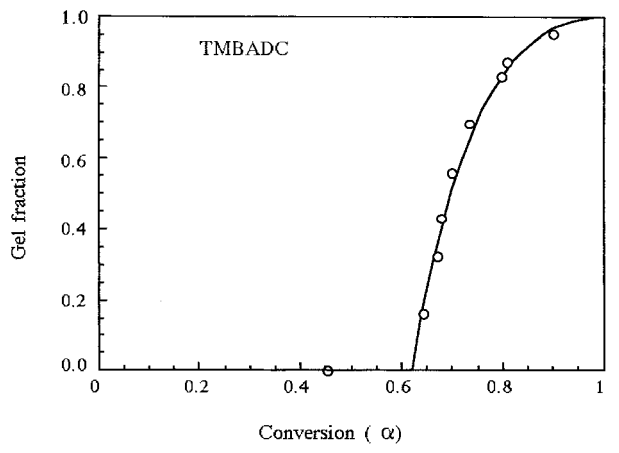

Figure 3 Comparisons between the calculated gel fraction curve and the experimental TMBADC counterparts (symbols). The solid line is the calculated gel fraction curve by means of eq. (12) and $\alpha_{gel} = 0.62$.

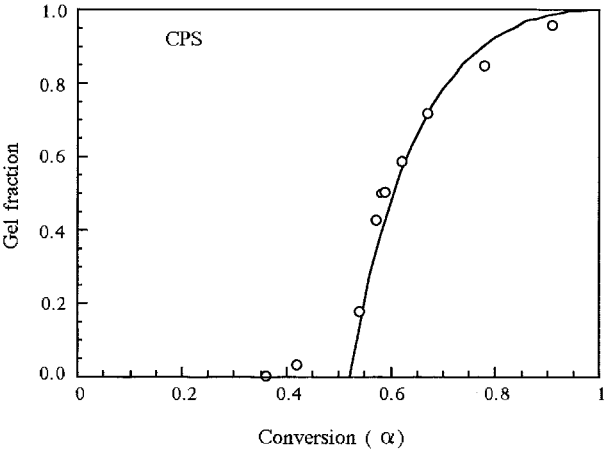

Figure 5 Comparisons between the calculated gel fraction curve and the experimental CPS counterparts (symbols). The solid line is the calculated gel fraction curve by means of eq. (12) and $\alpha_{gel} = 0.52$.

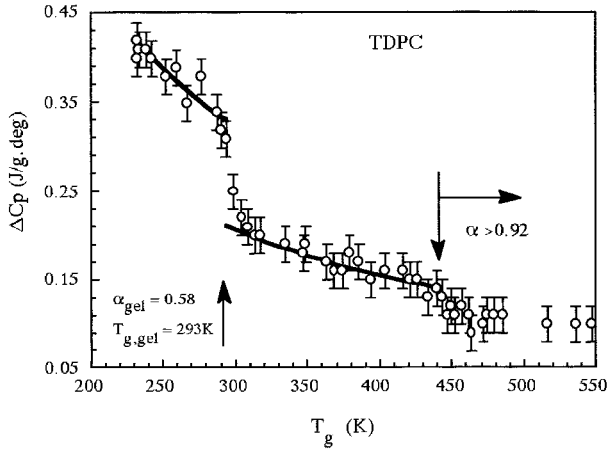

Figure 6 Plot of ΔC_p versus T_g for TDPC in various extent of cure. Symbols with the error bar are the experimental data. The solid line follows $\Delta C_p \cdot T_g = 97$ J/g in the pre-gel regime, and $\Delta C_p \cdot T_g = 62$ J/g in the post-gel regime.

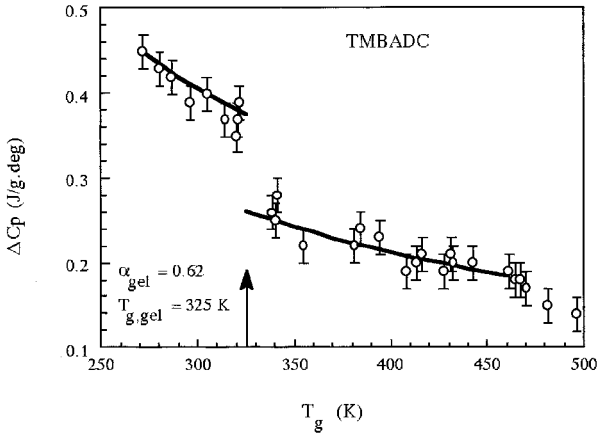

Figure 8 Plot of ΔC_p versus T_g for TMBADC in various extent of cure. Symbols with an error bar are the experimental data. The solid line follows $\Delta C_p \cdot T_g = 122$ J/g in the pre-gel regime, $\Delta C_p \cdot T_g = 85$ J/g in the post-gel regime.

observed for some systems in high conversion part ($\alpha > 0.92$ or higher), but the reason was unclear.

The drop-off in the $\Delta C_p \cdot T_g$ value at the gel point may arise in three possible ways. The first possible way is that both the ΔC_p and T_g have discontinuity in the vicinity of gel conversion. The second possible way is that only one among ΔC_p and T_g, there is discontinuity at the gel point. Another possible way is the combined result of product $\Delta C_p \cdot T_g$ value. To examine the possible clue, we plotted the T_g conversion dependence first. Shown in Figures 10–13 are the plots of T_g versus α for TDPC, BADC, TMBADC, and HFBADC, respectively. The solid line in each figure is the fitting result from the restated DiBenedetto equation,[5,6,36] as follows:

$$\frac{T_g - T_{go}}{T_{g\infty} - T_{go}} = \frac{\lambda\alpha}{1 - (1 - \lambda)\alpha} \tag{15}$$

where λ is the fitting parameter. T_{go} and $T_{g\infty}$ refer to the glass transition temperature at $\alpha = 0$

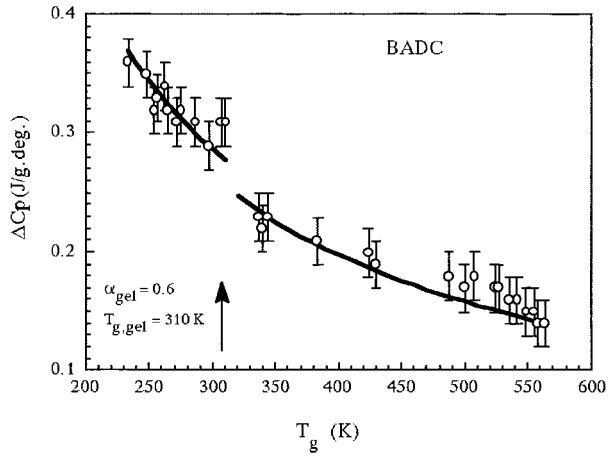

Figure 7 Plot of ΔC_p versus T_g for BADC in various extent of cure. Symbols with error bar are the experimental data. The solid line follows $\Delta C_p \cdot T_g = 86$ J/g in the pre-gel regime, $\Delta C_p \cdot T_g = 79$ J/g in the post-gel regime.

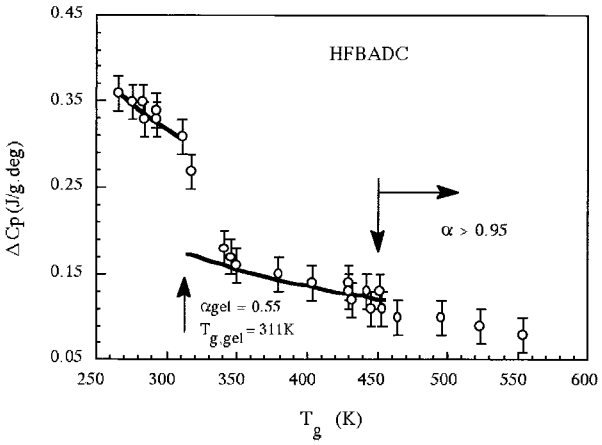

Figure 9 Plot of ΔC_p versus T_g for HFBADC in various extents of cure. Symbols with an error bar are the experimental data. The solid line follows $\Delta C_p \cdot T_g = 95.4$ J/g in the pre-gel regime, and $\Delta C_p \cdot T_g = 54.5$ J/g in the post-gel regime.

Table II Summary of $\Delta C_p \cdot T_g$ Values for Various Structures of Aromatic Dicyanates

	Pre-Gel Region $\Delta C_p \cdot T_g$ (J/g)	Post-Gel Region $\Delta C_p \cdot T_g$ (J/g)	$T_{g,\text{gel}}$ (K)	α_{gel}
TDPC	97	62	293	0.58
BADC	86	79	310	0.60
HFBADC	95.4	54.5	311	0.55
TMBADC	122	85	325	0.62

(monomer state) and at $\alpha = 1$ (fully cured state), respectively. λ are obtained 0.162, 0.242, 0.205, and 0.15 for TDPC, BADC, TMBADC, and HFBADC, respectively. Smooth results were observed from the fitting curves and experimental counterparts. No significant break occurs in the $T_g - \alpha$ dependence curve at the gel point, implying there should be a big change in the $\Delta C_p - \alpha$ dependence curve in the vicinity of gel conversion to respond the fact that the product $\Delta C_p \cdot T_g$ has a drop-off value at that point. Shown in Figure 14 is a representative plot of ΔC_p versus α for TDPC (the other specimen were not shown for brevity).

DISCUSSION

Intramolecular cyclization always accompanies intermolecular crosslinks. Dusek and MacKnight[37] suggested that the intensity of intramolecular cyclization depends on the structure of the constituent units and very much on the reaction mechanism. If the network is built from low functionality component, intramolecular cyclization is relatively weak. On the contrary, highly intramolecular cyclized products may be obtained from a high functionality component. One sym-triazine ring is formed for each cyclotrimerization of aromatic dicyanates. For each *sym*-triazine ring formed, two additional unreacted sites are formed on the parent molecule. A vast number of unreacted sites on one molecule (like a high functionality component) easily yield a certain level of intramolecular cyclization. That is the real reason why the gel conversion was much delayed and cannot be predicted by the mean-field theory in those aromatic dicyanate systems.

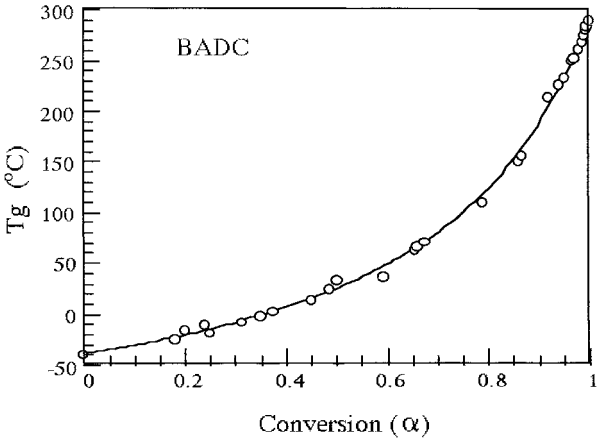

Figure 11 Plot of T_g versus conversion for BADC. Symbols represent the experimental data. The solid line is the fitting result by eq. (15) with $\lambda = 0.242$.

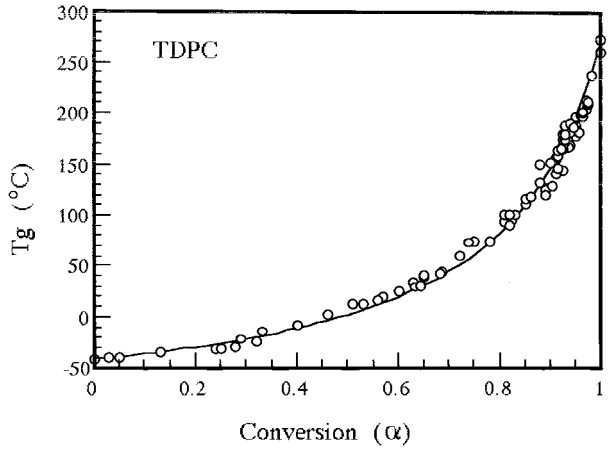

Figure 10 Plot of T_g versus conversion for TDPC. Symbols represent the experimental data. The solid line is the fitting result by eq. (15) with $\lambda = 0.162$.

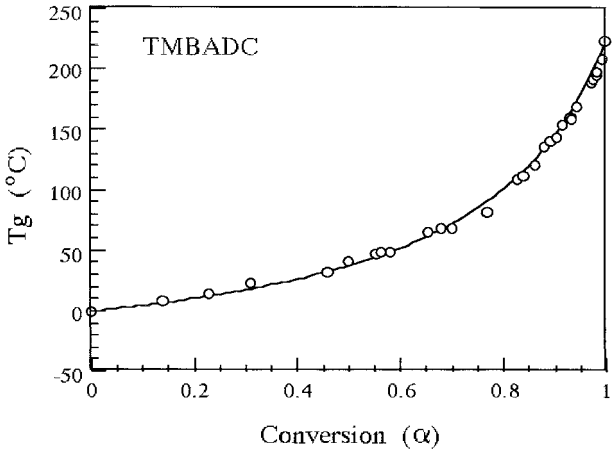

Figure 12 Plot of T_g versus conversion for TMBADC. Symbols represent the experimental data. The solid line is the fitting result by eq. (15) with $\lambda = 0.205$.

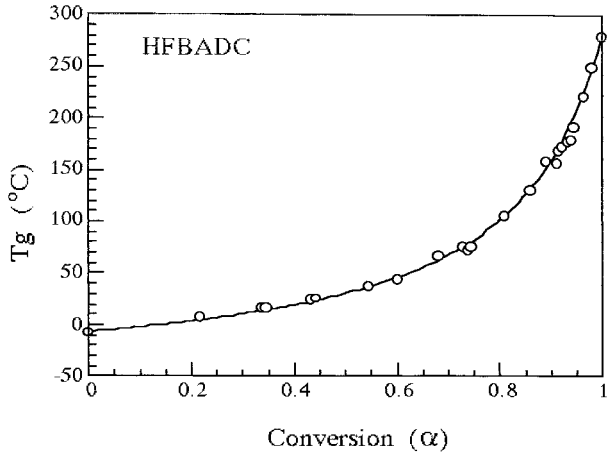

Figure 13 Plot of T_g versus conversion for HFBADC. Symbols are the experimental data. The solid line is the fitting result by eq. (15) with $\lambda = 0.15$.

In the Monte Carlo study of Gupta and Macosko,[1] it was found that $\alpha_{gel} = 0.5$ (which is the mean-field result) for an allowed reaction radius (R_h) of four monomer sizes; if $R_h = 2$ monomer sizes, $\alpha_{gel} = 0.68$ (These results were obtained by permitting intracluster cyclization in the computer simulation). It was concluded that limited accessibility should be the main reason of the delayed gelation in the latter case. Imposing a further restriction, disallowing intramolecular cyclization for the case of $R_h = 2$ monomer sizes, they observed a shift of α_{gel} from 0.68 to 0.56, indicating that two-thirds of the delay in gelation actually came from intramolecular cyclization. In other words, effect of intramolecular cyclization is strongly enhanced in the presence of limited accessibility. The limited accessibility, in the sense, is the rigidity in local packing, which is responsible for the presence of buried, unreacted group and not the global diffusion of cluster in the system. This limited accessibility should be also not the diffusion limitation in the vitrification process as the glass transition temperature (T_g) of the thermosetting system approaches the reaction temperature. For TDPC, T_g is approximately 20°C at $\alpha_{gel} = 0.58$, which is more than 130°C below the reaction temperature.

BADC was chosen as the standard specimen due to its structure and to the fact that a few of reported values of gel conversion could be taken as reference.[1,6] Gel conversion of BADC was found at 0.60 ± 0.01, in good agreement with the previously reported values. As compared with BADC, TMBADC has two additional pendent groups (—CH_3) on both sides of each functional group, which result in a steric hindrance effect, thereby decreasing the accessibility of functional groups. The gel fraction (ϕ_{gel}) of TMBADC was expectedly obtained at $\alpha_{gel} = 0.62$, higher than that of BADC due to the decrease in the accessibility of functional groups. Also as compared with BADC, CPS has a long and flexible chain segment between the two functional sites, which increases the feasibility of chain end diffusion and, hence, the increase in the accessibility of functional sites. Meanwhile, the long chain segment may result in the less intramolecular cyclization. Therefore, for CPS, a lower value of α_{gel} ($\alpha_{gel} = 0.52$) than that of BADC would be reasonably expected. It may be concluded that different intensity of intramolecular cyclization should be responsible for different degree of delayed gelation.

The substitution effect was investigated by HFBADC, which has strong electron withdrawing groups (—CF_3) in the backbone. Gelation was observed at earlier conversion ($\alpha_{gel} = 0.55$) than that of BADC, implying that the positive substitution effect indeed influence the gel conversion. On the other hand, the substitution effect may also influence the intensity of intramolecular cyclization. The positive substitution effect may induce the unreacted sites on the parent molecule more active. Because the larger molecules have larger amount of more active unreacted sites, these larger molecules are easy to react mutually, thereby developing outwards. Accordingly, less intensity of intramolecular cyclization is obtained for HFBADC due to the positive substitution effect. Therefore, gelation of HFBADC was ob-

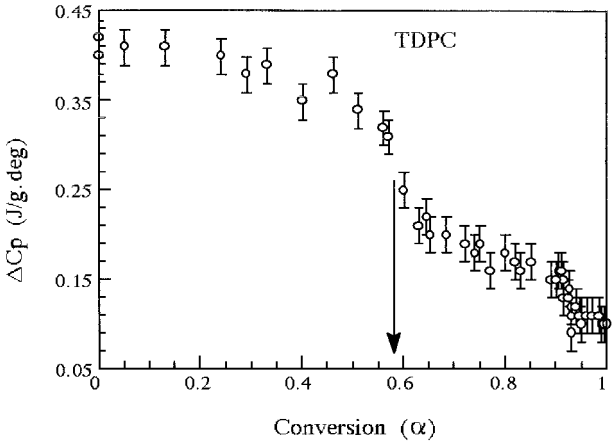

Figure 14 Plot of ΔC_p versus conversion for TDPC. Symbols with error bar represent the experimental data. The marked arrow is the gel conversion.

served at earlier conversion (α_{gel} = 0.55) than that of BADC.

It should be reasonably inferred that intramolecular cyclization may play a dominant role in the dramatic change in gel conversion. The higher the extent of intramolecular cyclization the system has, the more delay of gelation. Therefore, we have developed some relevant expressions considering the intramolecular cyclization as an unique effect and expressed them as eqs. (12) and (14). Consequently, the experimental counterparts (symbols) in Figures 2–5 (different structures of constituent units) were excellently fitted by means of eq. (12) and the corresponding α_{gel}.

It should be pointed out that one would expect to see a more pronounced increase in T_g after the gel point since the elastically effective crosslink density remains null before the gel point and starts rising immediately thereafter. In our systems, however, we do not observe such a break at the gel point in Figures 10–13. The possible explanations are as follows. Firstly, the gel fraction can be measured only at a long-range change in the molecular crosslinking associated with spatial structure in the system; therefore, the gel fraction is not sensitive to the intramolecular cycles. Whereas the observed T_g is a relaxation phenomenon associated with a relatively small number of segments; therefore, observed T_g can be continuously contributed by the intramolecular cycles. Alternatively, the contribution of crosslinked junctions within intramolecular cycles to the gelation may be too small to detected, but intramolecular cycles are indeed present and confine the mobility of molecular segments (can be considered as increasing amount of branch points), thereby continuously promoting T_g, and, hence, no obvious break point at gel point was observed. In other word, any crosslinks, whether elastically effective or not, should offer the same contribution to T_g.[38]

A dramatic change in the product value of $\Delta C_p \cdot T_g$ was found in the vicinity of the gel point for all different structures of aromatic dicyanate systems. It means that there are entirely different values of $K_1^2V/\Delta\beta$ [eq. (3)] between the pre-gel and post-gel regimes. We don't know precisely which factor plays the dominant role in determining the different values of $\Delta C_p \cdot T_g$ between two regimes. From the direct experimental observation, $T_g - \alpha$ dependence curves show no break point over the whole range of conversion, and $\Delta C_p - \alpha$ curves exhibit a significant drop-off in the vicinity of gel point. The dramatic change in $\Delta C_p \cdot T_g$ occurs at the gel point rather than the expected mean-field gel conversion of 0.5, presumably due to the intramolecular cyclization. Only elastically effective crosslinks appreciably confine the number of holes to go through the glass transition, thereby yielding a much smaller value of ΔC_p. Crosslinked junctions within intramolecular cycles are not very effective to confine the number of holes to go through the transition; hence, the value of ΔC_p still remains at high level in the pre-gel regime.

CONCLUSIONS

Polycyclotrimerization of aromatic dicyanate system behaves like the reaction of high functionality monomer, which easily undergoes the intramolecular cyclization. That is real reason why the gel conversion is much delayed from mean-field value of 0.5 to the real value of approximately 0.58 to 0.65. The extent of delayed gelation depends on the monomer structure associated with the accessibility of the functional group, the substitution effect, and the effect of the intramolecular cyclization during the polycyclotrimerization. These effects are not independent events, the former two effects can be quantitatively represented in terms of the extent of the intramolecular cyclization. The theoretical expressions [eqs. (9), (10), (12), and (14)] were derived by use of the recursive method with due consideration of intramolecular cyclization. Equations (9), (10), and (12) were found to be effective in describing gel fraction-conversion data for various polycyanurates, whereas eq. (12) was much simpler (with only one experimental parameter, α_{gel}) and without loss of generality in use. A dramatic change in the product value of $\Delta C_p \cdot T_g$ was also found in the vicinity of gel point for all the different structures of aromatic dicyanate systems, presumably due to the same reason as that of delayed gelation.

The financial support of the National Science Council under contract number NSC-87-2216-E-151-002 is grateful acknowledged.

REFERENCES

1. Gupta, A. M.; Macosko, C. W. Macromolecules 1993, 26, 2455.

2. Miller, D. R.; Macosko, C. W. Macromolecules 1976, 9, 206.
3. Fukui, K.; Yamabe, T. J Polym Sci 1960, 45, 305.
4. Georjon, O.; Galy, J.; Pascault, J. P. J Appl Polym Sci 1993, 49, 1441.
5. Mirco, V. R.; Cao, Z. Q.; Mechin, F.; Pascault, J. P. Polym Mater Sci Eng 1992, 66, 451.
6. Osei-Owusu, A.; Martin, G. C.; Gotro, J. T. Polym Mater Sci Eng 1991, 65, 304.
7. Osei-Owusu, A.; Martin, G. C.; Gotro, J. T. Polym Mater Sci Eng 1992, 32, 535.
8. Chen, Y. T.; Macosko, C. W. Proceedings of the 24th International SAMPE Symposium, Toronto, Ontario, Canada, 1992.
9. Simon, S. L.; Gillham, J. K. Polym Mater Res Eng 1992, 203, 231.
10. Simon, S. L.; Gillham, J. K. Polym Mater Sci Eng 1992, 66, 502.
11. Simon, S. L.; Gillham, J. K. J Appl Polym Sci 1993, 47, 461.
12. Armistead, J. P.; Snow, A. Polym Mater Res Eng 1992, 203, 233.
13. Armistead, J. P.; Snow, A. Polym Mater Sci Eng 1992, 66, 457.
14. Liu, H.; George, G. A.; Halley, P. J. Polymer 1997, 38, 2997.
15. Lu, M. C.; Hong, J. L. Polymer 1994, 35, 2822.
16. Korshak, V. V.; Pankratov, V. A.; Ladovskaya, A. A.; Vinogradova, S. V. J Polym Sci, Polym Chem 1978, 16, 1697.
17. Gupta, A. M. Macromolecules 1991, 24, 3459.
18. Gupta, A. M.; Hendrickson, R. C.; Macosko, C. W. J Chem Phys 1991, 95, 2097.
19. Miller, D. R.; Macosko, C. W. Macromolecules 1980, 13, 1063.
20. Bauer, J.; Bauer, M. Acta Polym 1987, 38, 16.
21. Bauer, J.; Bauer, M. J Macromol Sci 1990, A27(1), 97.
22. Lin, R. H. Ph.D. Dissertation, Institute of Material Science and Engineering, National Sun Yet-Sen University, Taiwan, 1996.
23. Lin, R. H.; Hong, J. L.; Su, A. C. Polymer 1995, 36, 3349.
24. Simha, R.; Boyer, R. F. J Chem Phys 1962, 37, 1003.
25. Sperling, L. H. Introduction to Physical Polymer Science, 2th Ed.; John Wiley & Sons: New York, 1993; pp. 334–337.
26. Nose, T. Polym J 1971, 2, 437.
27. Sperling, L. H. Introduction to Physical Polymer Science, 2th Ed.; John Wiley & Sons: New York, 1993; pp. 343–345.
28. Wunderlich, B. J Phys Chem 1960, 64, 1052.
29. Richardson, M. J.; Savill, N. G. Polymer 1975, 16, 753.
30. Grigat, E.; Putter, R. Chem Ber 1964, 97, 3012.
31. Macosko, C. W.; Miller, D. R. Macromolecules 1976, 9(2), 199.
32. Simon, S. L.; Gillham, J. K. J Appl Polym Sci 1993, 47, 461.
33. Nielsen, L. E. J Macromol Sci, Rev Macromol Chem 1969, C3, 69.
34. Hale, A.; Macosko, C. W.; Bair, H. E. Macromolecules 1991, 24, 2610.
35. Lin, R. H.; Hong, J. L.; Su, A. C. Comput Theor Polym Sci 1997, 7, 95.
36. Pascault, J. P.; Williams, R. J. J. J Polym Sci, Polym Phys Ed 1990, 28, 85.
37. Dusek, K.; MacKnight, W. J. in Cross-linked Polymer Chemistry, Properties and Application; ACS Symposium Series 367; American Chemical Society, Washington DC., 1988; pp. 2–27.
38. Stutz, H.; Illers, K. H.; Mertes, J. J Polym Sci, Polym Phys Ed 1990, 28, 1483.